International Journal of Computer Information Systems and Industrial Management Applications
ISSN 2150-7988 Volume 18(2) 2026 pp. 1961-1975
https://doi.org/10.70917/ijcisim-2026-5281
Article

Enhanced Brain Tumor Classification Using Capsule Networks with Hybrid Activation Function

Mamta Sharma[1*], Sunita Beniwal[2]

[1]Department of Computer Science and Engineering, Guru Jambheswar University of Science & Technology, Hisar and Department of Computer Science and Engineering, Shree Guru Gobind Singh Tricentenary University, Gurugram
[2]Department of Computer Science and Engineering, Guru Jambheswar University of Science &Technology
*mamtash.220@gmail.com

Abstract: Detection of life-threatening disease at an early stage is crucial for improving patient survival rates. The advancement in diagnostic technology has made disease identification faster and more accurate. Brain tumors are very critical and require prompt and precise detection for treatment. Deep learning algorithms can aid medical experts in diagnosis and treatment. Capsule Networks, a Deep Learning technique, have shown significant potential in medical diagnosis. The performance of capsule networks is driven mainly by the choice of activation functions, as Activation functions help in improving sensitivity to detect the spatial and orientational rotation. In this study, a hybrid activation function combining ReLU and Swish is proposed to make a more effective activation function. The proposed model achieves an accuracy of 96.83%, precision of 96.84%, recall of 96.83%, and a ROC value of 98.07%. Comparative analysis shows that the proposed approach performs better than the other state-of-the-art techniques, highlighting its effectiveness in brain tumor detection.
Keywords: Brain Tumor, Activation Function, Capsule Networks, Deep Learning, MRI Images

1. Introduction

Emerging trends in the area of Artificial Intelligence are making it easier and smoother to detect life threatening diseases. Artificial intelligence interventions in medical diagnosis are quite impactful as it initiates automatic diagnosis, which is less error-prone than human examination [1]. AI has been widely used for detecting chronic diseases like covid, heart disease, kidney disease and various types of cancers, etc. in many cases, human experts are not able to find the root cause of an illness [2] and delayed detection can lead to severe consequences in some cases. Therefore, there is a need to find intelligent systems methods that provide accurate and rapid diagnosis. Artificial Intelligence helps to design intelligent systems.

Machine Learning, a subdomain of AI has been extensively used to diagnose the illness by finding patterns based on the symptoms and patient data. ML techniques can be classified broadly as supervised and unsupervised. [3]. The traditional ML techniques are not efficient enough to process unstructured data as well as it is not able to learn complex features without human interventions [4]. To overcome these drawbacks, Deep Learning techniques are used. These techniques utilize a number of hidden layers between the input stage and output stage to learn complex features making them effective for disease diagnosis [5].

Brain tumor is one of the critical diseases, impacting central nervous system.[6]. It is a condition in which the brain stops normal functioning. The brain is the most complex organ of the human body controlling vital functions in the body. Deposition of lumps or mass in the brain is called as brain tumor. Such abnormalities can affect overall functioning of the body and if not treated on time this condition can become life threatening.

There are many alternatives that are used by medical practitioners to collect samples from the patients to analyze and examine the brain tissues to reach a certain result. One of the most commonly used options is medical imaging. Commonly used image modalities that help the medical experts are MRI [7], CT-scan, PET, and EEG. MRI is the most preferred method out of these because of its non-invasive nature as it enables detailed visualization of brain [8]. Figure 1 shows the sample MRI images from a dataset for brain tumor analysis.

MRI is of commonly classified into following categories T1, T2, and 3D-Flair[9]. Deep Learning techniques predominantly used for MRI inspection are CNN, VGGNET, ALEXNET, YOLO, DENSNET, etc. among these CNN is the most widely used for MRI based diagnosis due to its ability in studying image data and giving rapid results [10][11].

One of the disadvantages generally faced by CNN is its resistance to image orientation. CNN fails to detect the features of images efficiently when the images are rotated or flipped thus hampering the efficiency of the CNN and the outcomes are not as expected due to its max-pooling layer.

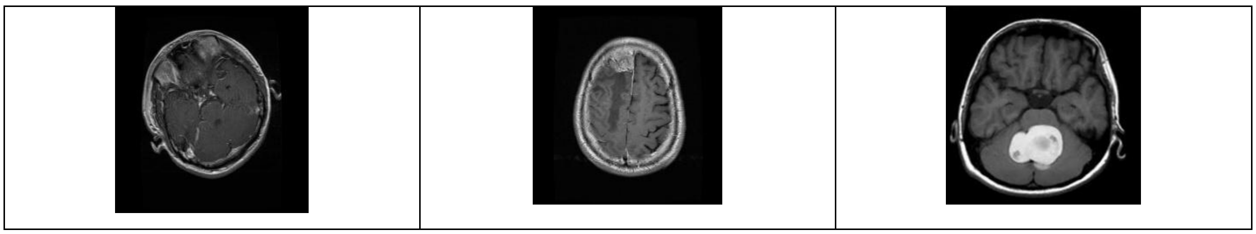

Fig 1. The MRI image of Brain Tumor

Most of the techniques that are present today generally use ReLu, Tanh, Swish, Leaky Relu, Sigmoid activation functions individually. Relu is very effective computationally, but it generally suffers from inactive neurons and low gradient flow. Swish counters this disadvantage of the ReLU activation function. So, better results can be achieved by integrating activation functions. To overcome the limitations of the individual activation function, i.e., ReLU, Leaky ReLU, and PReLU. The proposed hybrid activation function helps to simplify the computational complexity and sparsity of ReLU together with the smooth optimization behavior of Swish. This work improves the representation of nonlinear features.

To overcome this disadvantage, Capsule Networks have been introduced. Capsule networks are a subset of CNN [12] using dynamic routing instead of the max-pooling layer of the CNN and this enables Capsule Networks to detect the features of the rotated images. So Capsule networks shows better performance in identifying images with varying orientations. Also, the activation function in the capsule networks plays a crucial role in the efficiency of capsule networks. In this work a hybrid activation function is proposed used to improve the overall performance.

The remaining paper is organized as follows: section 2 presents the literature review, section 3 explains the proposed methodology, followed by results and finally conclusion.

2. Literature Review

Detection and classification of brain tumors using MRI images have been widely studied in recent years. This section reviews the existing work on brain tumor detection using machine learning and deep learning approaches. It also covers application of capsule networks and various activation functions along with their impact to improve the classification results.

Discriminative feature extraction using deep learning techniques has increased classification accuracy of brain tumors on MRI images. The ability of capsule networks to work on images with different orientations has made their use in brain tumor classification more efficient. Researchers have focused on Capsule networks and various activation functions. Afshar et al. [19] classified brain tumor using CAPSNET and reported an efficiency of 86.56% for the proposed technique which outperformed CNN that has an accuracy of 72.13%. Adu et al. [13] proposed an activation function named parametric scaled hyperbolic tangent (PSTanh), which improved the tanh function by addressing vanishing gradients. They compared the proposed technique with eight existing techniques of activation optimization and reported that the proposed function outperformed all the other activation function with an accuracy of 96.70%. Gagana et al. [14] compared the different existing activation functions by applying these on MNIST dataset and observed that the e-swish function outperformed both ReLU and PreLU with an accuracy of 99.56%. Xi et al. [15] explored the capsule networks with increased complexity of the dataset. They increased stacking and primary capsules to deal with the complexity and modified the restructuring loss. And on CIFAR and MNIST datasets 71.50% was the maximum achieved accuracy. Punjabi et al. [16] compared the efficiency of the capsule network in the field of rotating object visualization with CNN. To compare the features of CNN and capsule networks, deep visualization was done to examine how well the capsule networks analyze the changes in visual alterations. Afshar et al. [20] proposed a technique using modified capsule networks to classify Brain tumor for coarse boundaries to overcome the disadvantage of the conventional Capsule networks and reported that advanced technique was able to achieve the accuracy of 90.89%. Kumar et al. [21] has given a segmentation method using attention mechanism and dynamic routing for the Brain Tumor classification. The performance criteria used were Dice Coefficient and Housdorff distance for different sample sizes and reported better performance than other techniques.

Akinyelu et al. [22] reviewed ML, DL, CNN, CapsNet etc. which are widely used to predict brain tumor. All the existing activation functions were studied and reviewed by Hammad [23] along with the need of the activation functions, suitability of different activation function for various tasks, and the advantages and disadvantages. Kumar et al. [17] presented a systematic review of impact of deep learning on image analysis and its classification. They covered the DL techniques that are used predominantly in the image classification like CNN, Transfer learning, LSTM, GAN etc.

CNN models have been used on MRI images for feature selection and classification. Research shows that feature selection using CNN performs better than manual feature selection [18,34,24]. Deep learning models have been shown to improve classification on multi-class and complex tumors [25,27,28]. Mokri et al. [18] proposed a CNN based deep learning technique using Python language for classification of BT for three classes i.e., glioma, meningioma, pituitary brain tumor and showed that automated feature extraction using CNN gave better results than manual feature extraction. Mahjoubi et al. [34] performed feature extraction using CNN to classify MRI images of multiple tumor classes which appeared similar and they reported improved classification performance. Hossain et al. [24] integrated CNN and KNN using CNN layers for automatic feature extraction and KNN for classification. They reported that their approach performed better than traditional classifiers and CNN alone. Kumar et al. [25] evaluated machine learning algorithms with various feature selection techniques and reported that classification performance is decided by the discriminative ability of features used. Mahmud et al. [27] used CNN on MRI images and reported that for multi-class classification, deep learning models outperform traditional models. Woźniak et al. [28] used deep neural networks with correlation learning on brain tumor CT images and were able to identify complex tumors using inter-feature dependencies with high accuracy.

Abnormalities in symmetry of brain and complex structure of brain makes it difficult for models to perform efficiently. Deep learning and optimization models have been used for improving performance on such images [26,29]. Al-Azawi [26] analysed the symmetry of brain for finding the abnormality by comparing the difference in left-right hemispheres of MRI images using symmetry-based abnormality identification. However, the rule-based technique used by them was not able to work efficiently on images with bilateral tumors, surgery induced changes, and genetic abnormalities. Khalil et al. [29] used dragonfly optimization algorithm with level set segmentation and gave improved boundary delineation specifically for irregular tumors.

Issues like class imbalance and variation in patients have been shown to handled better using ensemble techniques [30,31]. Dudeja et al. [30] reported better classification accuracy and less variance than traditional systems using ensemble learning. They proposed EfficientNetB3 architecture for multi-class brain tumor classification. Kumar and Mohanty [31] also reported that ensemble models perform better than normal models when dealing with class imbalance problem and variation in patients. EFF_D_SVM model was developed by Zhang et al. [32] using effiecient net for extracting features and SVM for classification and showed better identification of multiple tumors. Transfer learning has also been used for predicting tumor stages and survival rate [33]. Rubio et al. (33) used transfer learning on glioma images for predicting stages and survival rates.

Table 1: Summary of the Existing work

Ref. No	Year	Techniques	Dataset	Performance
[24]	2024	Hybrid KCNN	3064 MRI Images	Accuracy: 89.99%
[25]	2024	Six Machine Learning techniques i.e. SVM, RF, LR, KNN, NB, DT	Three datastets from Kaggle	Accuracy: 99%
[26]	2022	Artificial Intelligence	300 images from standard dataset	Accuracy: 95.3%
[27]	2023	Deep Learning CNN, ResNet-50, VGG 16, Inception V3	Kaggle dataset	Accuracy: 93.30(CNN)
[28]	2021	CLM+CNN	3064 images from Kaggle.com	Accuracy: 96%
[29]	2020	Machine Learning: Random Forest, SVM	BRATS 2017	Accuracy: 98.2
[30]	2023	Ensemble EfficientNetB3	Kaggle Dataset with 3064 images	Accuracy: 99.24% DSC-0.914
[31]	2023	Different DL Models Densenet-121, Resnet-101 Mobilenet-V2	Kaggle Dataset with 7023 images	Accuracy: DenseNet 121: 99%
[32]	2023	ML model: SVM with EEF-D for feature extraction	Chen Dataset-3064 images, Kaggle Dataset:3264 images	Accuracy: 98.96%
[33]	2023	Transfer Learning	BraTS 2020	Accuracy: 97%
[34]	2023	CNN	Kaggle Dataset	Accuracy: 95.44%
[35]	2022	ResNet50, InceptionV3 and MobileNet, VGG19	Kaggle Dataset	Accuracy: ResNet50, InceptionV3 MobileNet: 100%, Vgg19:99.7%
36	2025	Fuzzy Thresholding,optimized CNN	Kaggle Dataset	Accuracy: 98% , DCE: 97.97%

3. Methodology

This section presents the methodology adopted for the proposed experimental work. It describes the dataset used for the experiment, followed by pre-processing steps applied to the dataset to prepare the data for training the model. The dataset used for the experiment is in raw form and pre-processing is required to improve quality, consistency and suitability.

The dataset may have multiple deformities such as redundancy, missed values, noise, etc. which is why preprocessing is performed. After pre-processing, features are extracted to improve classification performance. The processed data is then divided into training, validation and testing subsets. Finally, the model is trained and evaluated on test data and the results are analyzed to assess its effectiveness.

Figure 2, shows the overall process flow for classification of the brain tumor. Initially data is collected, followed by pre-processing. After that features are extracted to enhance the performance of the model. The processed data is then provided to the model for the classification of brain tumor.

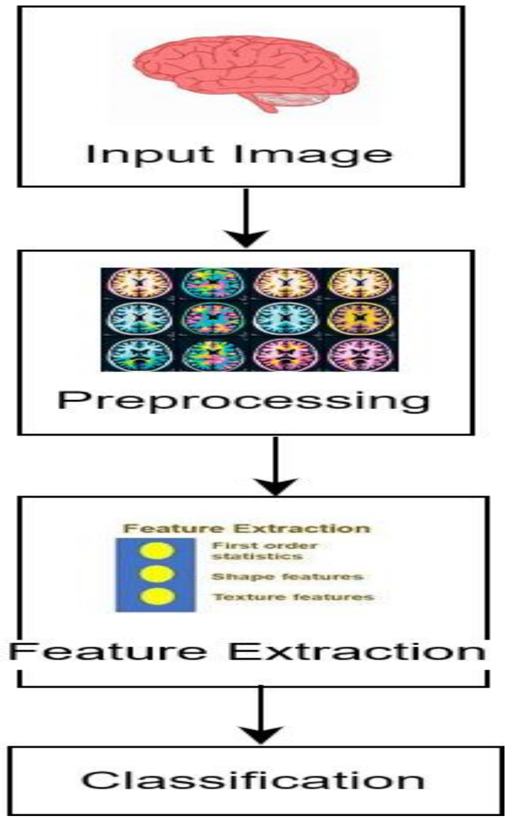

Figure 2. Process Flow Diagram for Classification

3.1 Experimental Setup:

The experiments were carried out in Google Colab environment using Python language. The system used was equipped with AMD Ryzen 5 7520U with Radeon Graphics processor. The Operating system used was Windows 11. The implementation used standard libraries and frameworks to efficiently train the model.

3.2 Hyperparameter Tuning:

The model is trained using selected hyperparameters to ensure optimal performance. The total number of epochs used were 125 with a batch size of 125 have been used for training. Adam optimized was used for optimization with learning rate of 0.001. The proposed hybrid activation function (ReLu -Swish) is utilized to improve model performance. The input image size used for the model is 125X125 pixels for maintaining the consistency.

3.3 Data Set Description

For the experiment, the brain tumor dataset that is used is obtained from Kaggle [36], which is an online source for research datasets. It has 3060 MRI images of brain. The images are divided into three different folders: Yes, No, and Pred.

The yes folder has the images with the yes label, i.e., the brain images that have a possible tumor.

The no folder has the images with the no label, i.e., the brain images with no tumor in it.

The pred folder contains the images used for prediction.

This image dataset is publicly available and widely used for experimental research, enabling effective evaluation and validation of proposed research work.

3.4 Dataset Preprocessing

The collected dataset is not directly suitable for classification and prediction as it may have certain issues like missing information, redundant image labels and noise or distortion. Therefore, it becomes necessary to pre-process the dataset to make it suitable for classification to ensure improved model performance.

The dataset used in this study is also preprocessed to clean and standardize the dataset. The images are rescaled to normalize the pixel range from [0,255] to [0,1] which helps in stabilizing and accelerating the training process. The images are normalized as defined in equation 1.

$$I_n(i,j) = \frac{I_r(i,j)}{255} \quad I_n(i,j) = \frac{I_r(i,j)}{255} \qquad (1) I_n(i,j) = \frac{I_r(i,j)}{255} I_n(i,j) = \frac{I_r(i,j)}{255}$$

where *In(i,j)* is the normalized image obtained after resizing the raw images at a scale of (0,255). *Ir(i,j)* represents the pixel intensity of raw image. This operation scales down the pixel values to [0,1], hence improving training stability and convergence.

Furthermore, all images are resized into a fixed size of (128 x 128) pixels to convert them into a uniform dimension. A batch size of 32 is considered for the training of the model. The number of epochs for training is 125. The dataset is split into train, test, and validation sets with ratios of 70%, 15%, and 15%, respectively.

3.5 Feature Extraction

After selecting and pre-processing the dataset, the next step is to extract features which is an important step for improving the image classification task. It involves identifying and selecting the most relevant and discriminative attributes from raw data or images to train the model effectively. In this study, CNN was used to extract the features. The input images are fed to a CNN, where a convolutional layer applies filters to capture patterns or specific features within a local area of interest. Pooling layers were used to reduce the spatial dimension. Among various pooling options, such as Min pooling, Max Pooling, Average Pooling, Max Pooling was used as it preserves the most important features while decreasing computational complexity.

3.6 Activation Function

In the proposed technique, a hybrid activation function is introduced. It combined two activation functions, i.e., Relu and Swish, to enhance model performance. The model was trained using this hybrid activation function and the results were compared with existing activation functions. The suggested activation function combines the sparsity and computing economy of ReLU with the smooth gradient features of Swish. To facilitate smooth gradient propagation and improve representation learning, the input feature map first undergoes the Swish transformation. After that, a ReLU operator is used to enforce sparse representations and remove negative activations. This sequential combination enables the model to benefit from rich feature learning and efficient computation, hence generalizing performance and improving classification.

3.6.1 ReLu Activation Function

The Rectified Linear Unit (ReLU) is commonly used activation function in deep learning because of its computational efficiency. It is defined as

$$f(y) = max(0, y) \qquad (2)$$

If input y is positive, then the output is same as input, otherwise it returns Zero. This helps in mitigating the vanishing gradient problem and accelerates convergence.

3.6.2 Swish Activation Function

A swish activation function is a non-monolithic smooth function that enhances gradient flow and improves learning.. It is defined as follows in Equation 3

$$f(y) = y.sigmoid(y) \quad (3)$$

In the above equation, the sigmoid is explained as follows in Equation 4

$$sigmoid(y) = \frac{1}{(1+e^{-y})} \quad (4)$$

Swish allows small negative values and provides better performance than ReLU in certain deep architectures.

3.6.3 Proposed Hybrid Activation Function

ReLu and Swish activation functions are merged to leverage the advantages of both in a sequential composition of Swish followed by ReLU..This is done to retain swish's smooth non-linearity while enforcing sparsity through ReLU.

Mathematical Formulation:

Let y be the input for the activation function. The hybrid function is defined as:

H(y)=ReLU(Swish(y))=max(0,y.sigmoid(y))

The hybrid activation function is explained in algorithm 1.

Algorithm 1: Hybrid Activation Function
Input: Assume y be the input tensor to the activation function, Output: Activated Tensor H(y). 1: For each element of y: Compute sigmoid: $sigmoid(y) = \frac{1}{(1+e^{-y})}$ Apply the Swish Activation Function $swish(y) = y.sigmoid(y)$ Apply ReLU: $\mathrm{ReLU}(y) = max(0, y)$ 2. Return f(y)
Final Expression: $H(y) = max(0, \frac{y}{1+e^{-y}})$

The proposed hybrid activation function can be explained with equation 5 given below:

$$H(x) = ReLu\big(Swish(x)\big) \quad (5)$$

Or

$$H(x) = max\big(0, y.\sigma(y)\big) \quad (6)$$

3.7 Dynamic Routing

Dynamic routing is the process used in capsule networks to predict how much one capsule's output contributes to capsules in the subsequent layer. Dynamic routing replaced the traditional max-pooling layer of CNN with a learnable, iterative routing mechanism that allows capsules to adaptively route information based on agreement. It is also known as routing by agreement that preserves spatial relationships and hierarchical features. In this lower level capsules generate prediction vectors for higher level capsules and these contributions are adjusted based on agreement between these predictions and actual output of higher level capsules. This agreement is mathematically explained in equation 7 given below:

$$a_{ij} = \hat{u}_{j|i} . v_j \tag{7}$$

where $\hat{u}_{j|i}$ is the prediction vector from capsule I to capsule j.

v_j is the output vector of capsule j.

a_{ij} is the dot product between the prediction and output.

This dynamic routing gives vector as an output that encode both feature presence and instantiation parameters enabling more robust feature representation than CNNs.

3.8 Classification

Once all the hyper tuning, data preprocessing and feature extraction is done, the final step is classification. In this study, Capsule Network were used for the classification task. The benefit of using capsule networks is that it can capture spatial relationships and orientation variations in images. Capsule networks can identify features of the images even if it is flipped or oriented because of dynamic routing or routing by agreement.

The proposed model used hybrid activation function with the capsule network architecture to enhance feature representation. Once the model classified the images the results were compared with the existing models. Figure 3 illustrates the architecture of proposed capsule network with a hybrid activation function.

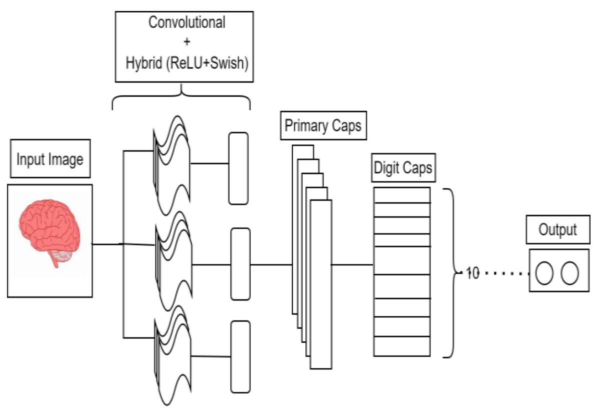

Fig 3. Capsule Networks Architecture with Hybrid Activation Function

4. Results and discussion

This section presents the results and comparison of the proposed model with existing techniques.

4.1 Evaluation Metrics:

To determine the effectiveness of the model, standard performance metrics including accuracy. precision, recall F1-score and ROC-AUC are used. These metrics shows the model's performance in terms of correctness, class discrimination and reliability. A brief description of these metrics is provided below:

Accuracy: It provides a simple measure of how well the model predicts outcomes. It is defined as ratio of correct classifications to total number of instances.

$$Accuracy = \frac{(T_n + T_p)}{(T_n + T_p + F_n + F_P)} \quad (8)$$

Precision: Precision is another important metric used to evaluate the effectiveness. It measures the proportion of correctly classified positive labels by the total of true positive and false positive. Precision is defined as:

$$Precision = \frac{T_p}{(T_p + F_p)} 2. \ (9)$$

Recall: Recall is used to evaluate the model's ability in correct classification of positive samples. It is calculated as ratio of true positives to total of false negatives and true positives. Recall is explained as equation 10

$$Recall = \frac{T_p}{F_n + T_p} \ (10)$$

F1-Score: F-1 score is used to provide a balanced evaluation by combining both precision and recall. It is particularly useful with imbalanced classes, as it considers both false positives and false negatives. It is determined by harmonic mean of precision and recall.

$$F - 1\ Score = \frac{2 \times precision \times recall}{Precision + recall} \quad (11)$$

ROC: The Receiver Operating Characteristic or ROC is a curve used to represent the performance of a classification model graphically. It is used to demonstrate the trade-off between the true positive rate and the false positive rate at different thresholds.

4.2 Performance of the proposed model:

Table 2 summarizes the performance of the proposed capsule network with hybrid activation function in terms of accuracy, precision, recall, ROC, and F-1 score.

Table 2: Performance of the proposed model

Proposed	Accuracy	Precision	Recall	ROC	F-1
ReLu+Swish	96.83%	96.84%	96.83%	98.07%	96.98%

From table 2, it can be observed that the proposed model has consistent performance across all metrics. The accuracy of 96.83% indicates strong prediction capability, while high precision and recall values demonstrate the model's effectiveness in minimizing both false positives and false negatives. ROC-AUC of 98.07% confirms the model's ability to distinguish between classes. An F-1 score of 96.98% indicates the model's excellent balance between precision and recall.

Figure 4 gives the confusion matrix of the proposed technique. It shows that the classes are divided proportionately and aligned with actual classes, indicating balanced and reliable performance.

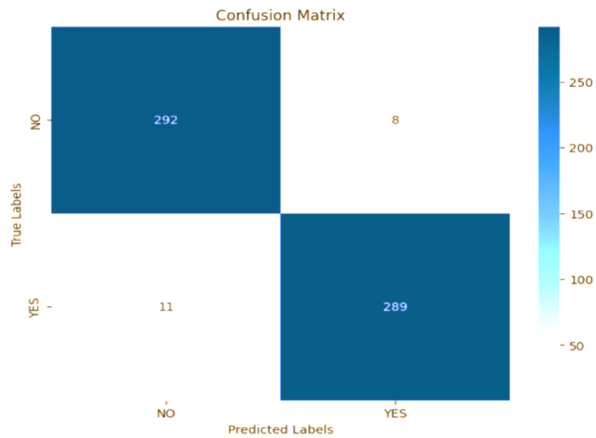

Figure 4 Confusion matrix obtained by the Proposed Model

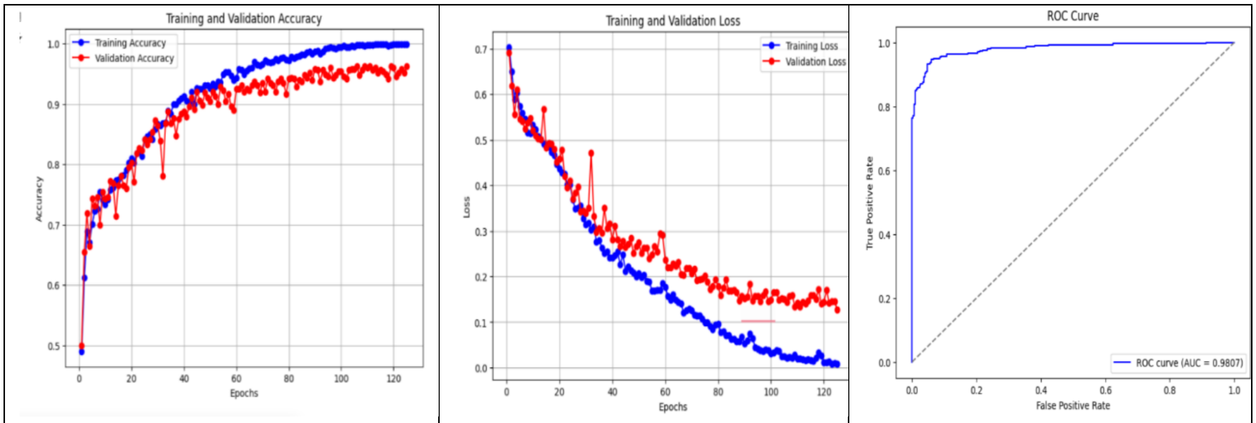

a) Training and Validation Accuracy	b) Training and Validation Loss	c) ROC-AUC curve

Figure 5: Performance of CapsNet using proposed activation function

Figure 5 a) presents the training and validation accuracy curves of the proposed model, which show a consistent increase during the initial epochs, indicating that the model learns effectively from the data. The curves indicate the model's strong generalization capability without much overfitting. Similarly, the loss curves presented in Figure 5 b) show a decrease in both validation and training loss, indicating that the model learns effectively and minimizes errors. The loss curves demonstrate stable convergence and good generalization of the model. ROC-AUC curve of the proposed technique, shown in Figure 5 c), indicates the model's discriminative capability with high TPR and minimal FPR. An AUC value of 98.07% reflects excellent classification capability to distinguish between tumor and non-tumor classes.

Overall, the proposed model demonstrates strong generalization ability, high predictive performance and stable convergence.

4.3 Ablation Study: Effect of Activation Functions

To evaluate the effectiveness of the proposed hybrid activation function, a comparative analysis was done using ReLU, Swish, and the hybrid activation function.

ReLu: When ReLU activation function was applied, performance of the model has been illustrated in figure 6. Figure 6 a, b and c represents the accuracy, loss and ROC curves when ReLU activation function was used. The accuracy and ROC curves shows stable learning behaviour while loss curve indicates effective convergence. But the limitation is that dependence on ReLU alone lowered classification performance due to limited gradient flow as compared to the hybrid approach.

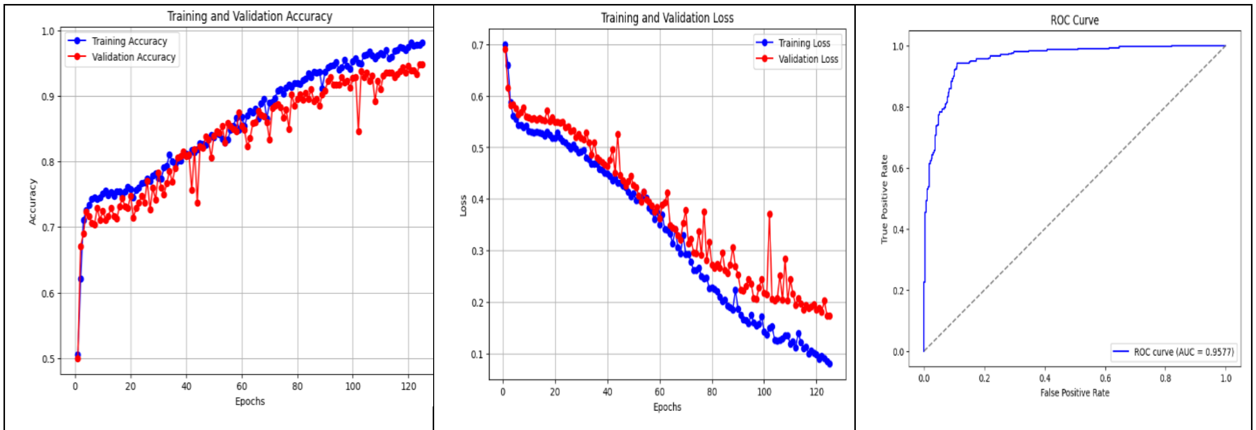

a) Training and Validation Accuracy	b) Training and Validation Loss	c) ROC-AUC curve

Figure 6: Performance of CapsNet using ReLU activation function

Swish: Performance of the model with the Swish activation function is shown in Fig. 7. Figure 7 a),b) and c) shows the accuracy, loss and ROC curves respectively. The performance of Swish was less consistent than ReLU, despite improved gradient propagation and small negative values being allowed. The accuracy and ROC-AUC values were lower, indicating the insufficiency of Swish alone in optimizing classification.

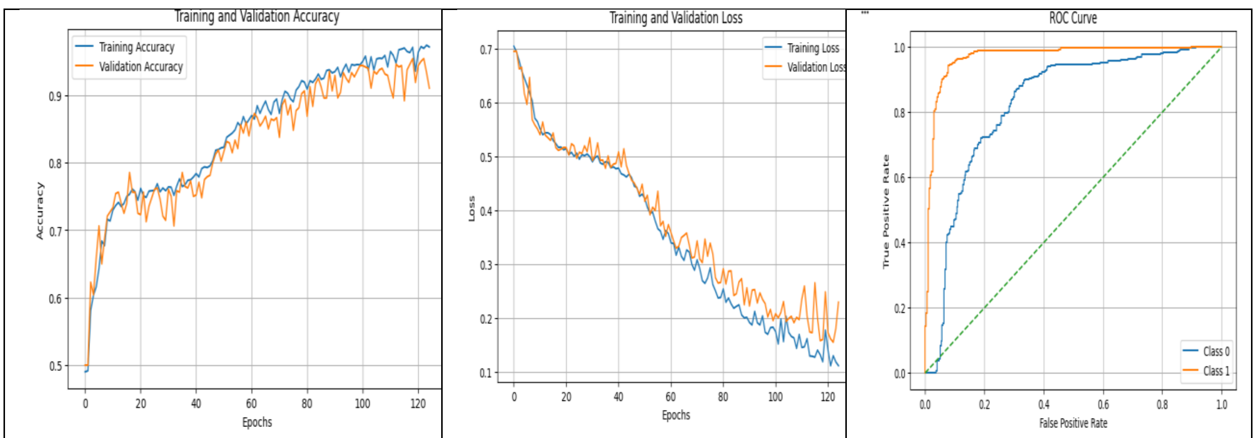

a) Training and Validation Accuracy	b) Training and Validation Loss	ROC-AUC curve

Figure 6: Performance of CapsNet using Swish activation function

Comparison of various activation functions:

Table 3 presents the comparative results. The results indicate it very clearly that the proposed hybrid activation function outperforms ReLU and Swish across all performance metrics. The hybrid activation function performs better due to its ability to combine the non-linear representation of Swish with the sparsity-inducing property of ReLU. Swish facilitates better gradient flow in deeper layers while ReLU suppresses negative activations, reducing noise and improving computational efficiency. This enhances feature representation in capsule networks, leading to improved classification performance.

Table 3: Comparison of the proposed activation function with Classical activation functions

Activation function	Accuracy	Precision	ROC-AUC	Recall
Relu	95.80	95.00	95.77	95.00
Swish	93.00	93.02	89.91	93.72
Sigmoid	77.49	76.23	80.01	76.64
Tanh	84.33	84.49	74.32	84.33
Leaky Relu	93.50	93.15	95.07	93.15
Relu+Swish	96.83	96.84	98.07	96.83

This ablation study confirms the main role of activation functions in capsule networks and demonstrates that the proposed hybrid ReLU–Swish function significantly improves classification performance. The results clearly indicate that the proposed hybrid activation function significantly improves classification performance by combining the strengths of ReLU and Swish.

Table 4. Performance of the Proposed Model Using 5-fold cross-validation

Metric	Mean	Standard Deviation (±)
Accuracy (%)	74.60	1.64
Loss	0.1623	0.0052
Precision (%)	75.66	2.25
Recall (%)	74.60	1.64
F1-Score (%)	74.35	1.55
AUC	0.8118	0.0161

Table 4 represents the performance of the proposed model, which is evaluated on the 5-fold cross-validation. The model achieved a mean classification accuracy of 74.60% ± 1.64%, with a precision of 75.66% ± 2.25%, recall of 74.60% ± 1.64%, and F1-score of 74.35% ± 1.55%. The proposed model also obtained an AUC of 0.8118 ± 0.0161. The low standard deviation indicates stable and consistent performance across validation folds.

Table 5. Statistical Comparison Between the Baseline CapsNet and the Proposed Hybrid ReLu-Swish CapsNet

Statistical Test	Statistic	p-value
Paired t-test	-12.2750	<0.001
Wilcoxon Signed-Rank Test	20.0000	<0.001

Table 5 represents the paired t-test and Wilcoxon signed-rank test. The paired t-test yielded a t-statistic of -12.2750 with a p-value < 0.001, indicating a statistically significant difference between the two models. Similarly, the Wilcoxon Signed-Rank Test produced a test statistic of 20.0 with a p-value < 0.001, confirming the significance of the improvement without assuming normality of the data.

Table 6. Confidence Interval Analysis

Parameter	**Value**
Mean Accuracy	74.60%
Standard Error	0.0082
Confidence Level	95%
Lower Confidence Limit	72.32%

Upper Confidence Limit	76.88%

Table 6 shows the confidence interval analysis of the proposed model. The model achieved a mean accuracy of 74.60%. and the standard error of 0.0082 has been achieved by the model. The 95% confidence interval with a lower limit 72.32% and upper limit76.88% indicates that the expected classification accuracy of the proposed model lies within this range with 95% confidence.

4.4 Comparative Analysis with Existing Models

To further validate the proposed technique, a comparative evaluation of the proposed model with several existing techniques, including SVM, logistic regression, decision tree, CNN and capsule network, is done and shown in Table 7. The results show that the proposed model achieved the highest accuracy and ROC-AUC among all models. SVM achieved slightly better recall. Traditional models like decision trees did not perform well due to their inability to capture spatial features in medical images. Deep learning models performed well but are not able to capture rotational invariance. Capsule networks overcome this through dynamic routing.

Table 7. Comparative analysis of Different Models

Model	Accuracy	Precision	Recall	ROC
DT	79.96	81.83	80.90	80.07
CNN	93.20	94.60	95.20	95.43
SVM	94.34	94.03	97.10	97.00
LR	95.01	95.65	96.76	97.89
CapsNet	95.50	95.02	96.20	98.00
Proposed	96.83	96.84	96.83	98.07

The improved performance of the proposed model over traditional models and CNN can be attributed to the capability of capsule networks to preserve spatial relationships and orientation information. Also, the use of a hybrid activation function enhances feature discrimination, resulting in improved classification performance.

5. Conclusion

As brain tumours are highly life-threatening, their timely and precise diagnosis is very important. In this study, an approach using capsule networks with a hybrid activation function is proposed for classifying brain tumors on MRI images. The results indicate that the proposed model is more accurate and reliable than other techniques across many evaluation parameters.

Despite its performance, the proposed model has certain limitations. The main limitation in implementing this method is the computational cost, driven by the complexity of capsule networks and dynamic routing. Another limitation is that the proposed approach was evaluated on a relatively smaller dataset. Efficiency can also be examined on larger datasets. The next limitation is that the proposed model focuses only on binary classification and has not been extended to multi-class classification. In future, the proposed model can be extended to larger datasets to evaluate its effectiveness. Improvements can be made to adapt the model to multi-class problems. Furthermore, it must be tested across modalities, including CT and PET. Efforts can be made to improve computational efficiency for real-time applications.

Conflicts of interest

The authors declare that they have no conflicts of interest.

Author contributions

The first author completed all the activities associated with literature review, development of ideas, formulation of the methodology, collection of the data, implementation of the system, evaluation of its outcomes, drafting of the manuscript, its corrections, and visualization. This work was to be supervised and feedbacked as well as the project managed by the second author.

REFERENCES

1. S. Kaur, J. Singla, L. Nkenyereye, S. Jha, D. Prashar, G. P. Joshi, and S. R. Islam, "Medical diagnostic systems using artificial intelligence (AI) algorithms: Principles and perspectives," *IEEE Access*, vol. 8, pp. 228049–228069, 2020. [CrossRef] [Google Scholar] [Publisher Link]
2. M. Tariq, Y. Hayat, A. Hussain, A. Tariq, and S. Rasool, "Principles and perspectives in medical diagnostic systems employing artificial intelligence (AI) algorithms," *Int. Res. J. Econ. Manag. Stud.*, vol. 3, no. 1, 2024. [CrossRef] [Google Scholar] [Publisher Link]
3. M. Cè, G. Irmici, C. Foschini, G. M. Danesini, L. V. Falsitta, M. L. Serio, and M. Cellina, "Artificial intelligence in brain tumor imaging: A step toward personalized medicine," *Current Oncology*, vol. 30, no. 3, pp. 2673–2701, 2023. [CrossRef] [Google Scholar] [Publisher Link]
4. S. F. Ahmed, M. S. B. Alam, M. Hassan, M. R. Rozbu, T. Ishtiak, N. Rafa, and A. H. Gandomi, "Deep learning modelling techniques: Current progress, applications, advantages, and challenges," *Artificial Intelligence Review*, vol. 56, no. 11, pp. 13521–13617, 2023. [CrossRef] [Google Scholar] [Publisher Link]
5. N. Ghaffar Nia, E. Kaplanoglu, and A. Nasab, "Evaluation of artificial intelligence techniques in disease diagnosis and prediction," *Discover Artificial Intelligence*, vol. 3, no. 1, Art. no. 5, 2023. [CrossRef] [Google Scholar] [Publisher Link]
6. K. Sailunaz, S. Alhajj, T. Özyer, J. Rokne, and R. Alhajj, "A survey on brain tumor image analysis," *Med. Biol. Eng. Comput.*, vol. 62, no. 1, pp. 1–45, 2024. [CrossRef] [Google Scholar] [Publisher Link]
7. P. K. Chahal, S. Pandey, and S. Goel, "A survey on brain tumor detection techniques for MR images," *Multimedia Tools Appl.*, vol. 79, no. 29, pp. 21771–21814, 2020. [CrossRef] [Google Scholar] [Publisher Link]
8. A. B. Abdusalomov, M. Mukhiddinov, and T. K. Whangbo, "Brain tumor detection based on deep learning approaches and magnetic resonance imaging," *Cancers*, vol. 15, no. 16, Art. no. 4172, 2023. [CrossRef] [Google Scholar] [Publisher Link]
9. M. Martucci, R. Russo, F. Schimperna, G. D'Apolito, M. Panfili, A. Grimaldi, and S. Gaudino, "Magnetic resonance imaging of primary adult brain tumors: State of the art and future perspectives," *Biomedicines*, vol. 11, no. 2, Art. no. 364, 2023. [CrossRef] [Google Scholar] [Publisher Link]
10. P. Tiwari, B. Pant, M. M. Elarabawy, M. Abd-Elnaby, N. Mohd, G. Dhiman, and S. Sharma, "CNN-based multiclass brain tumor detection using medical imaging," *Comput. Intell. Neurosci.*, vol. 2022, Art. no. 1830010, 2022. [CrossRef] [Google Scholar] [Publisher Link]
11. A. K. Agarwal, N. Sharma, and M. K. Jain, "Brain tumor classification using CNN," *Adv. Appl. Math. Sci.*, vol. 20, no. 3, pp. 397–407, 2021. [CrossRef] [Google Scholar] [Publisher Link]
12. Y. Liu, D. Cheng, D. Zhang, S. Xu, and J. Han, "Capsule networks with residual pose routing," *IEEE Trans. Neural Netw. Learn. Syst.*, 2024. [CrossRef] [Google Scholar] [Publisher Link]
13. K. Adu, Y. Yu, J. Cai, I. Asare, and J. Quahin, "The influence of the activation function in a capsule network for brain tumor type classification," *Int. J. Imaging Syst. Technol.*, vol. 32, no. 1, pp. 123–143, 2022. [CrossRef] [Google Scholar] [Publisher Link]
14. B. Gagana, H. U. Athri, and S. Natarajan, "Activation function optimizations for capsule networks," in *Proc. Int. Conf. Adv. Comput., Commun. Informatics (ICACCI)*, 2018, pp. 1172–1178. [CrossRef] [Google Scholar] [Publisher Link]
15. E. Xi, S. Bing, and Y. Jin, "Capsule network performance on complex data," *arXiv preprint arXiv:1712.03480*, 2017. [CrossRef] [Google Scholar] [Publisher Link]
16. A. Punjabi, J. Schmid, and A. K. Katsaggelos, "Examining the benefits of capsule neural networks," *arXiv preprint arXiv:2001.10964*, 2020. [CrossRef] [Google Scholar] [Publisher Link]
17. R. Kumar, P. Kumbharkar, S. Vanam, and S. Sharma, "Medical images classification using deep learning: A survey," *Multimedia Tools Appl.*, vol. 83, no. 7, pp. 19683–19728, 2024. [CrossRef] [Google Scholar] [Publisher Link]
18. S. M. G. Mokri, N. Valadbeygi, and V. Grigoryeva, "Diagnosis of glioma, meningioma and pituitary brain tumor using MRI images recognition by deep learning in Python," *EAI Endorsed Trans. Intell. Syst. Mach. Learn. Appl.*, 2024. [CrossRef] [Google Scholar] [Publisher Link]
19. P. Afshar, A. Mohammadi, and K. N. Plataniotis, "Brain tumor type classification via capsule networks," in *Proc. IEEE Int. Conf. Image Process. (ICIP)*, 2018, pp. 3129–3133. [CrossRef] [Google Scholar] [Publisher Link]
20. P. Afshar, K. N. Plataniotis, and A. Mohammadi, "Capsule networks for brain tumor classification based on MRI images and coarse tumor boundaries," in *Proc. IEEE ICASSP*, 2019, pp. 1368–1372. [CrossRef] [Google Scholar] [Publisher Link]
21. M. Kumar, J. Ramasamy, M. P. Kumar, and B. K. Harsha, "An improved segmentation method for brain cancer using capsule neural networks," *ICTACT J. Image Video Process.*, vol. 13, no. 4, 2023. [CrossRef] [Google Scholar] [Publisher Link]

22. A. A. Akinyelu, F. Zaccagna, J. T. Grist, M. Castelli, and L. Rundo, "Brain tumor diagnosis using machine learning, convolutional neural networks, capsule neural networks and vision transformers applied to MRI: A survey," *J. Imaging*, vol. 8, no. 8, Art. no. 205, 2022. [CrossRef] [Google Scholar] [Publisher Link]
23. M. M. Hammad, "Deep learning activation functions: Fixed-shape, parametric, adaptive, stochastic, miscellaneous, non-standard, ensemble," *arXiv preprint arXiv:2407.11090*, 2024. [CrossRef] [Google Scholar] [Publisher Link]
24. M. M. Hossain, M. M. Hasan, S. Khandaker, A. Islam, and N. Sulaiman, "Brain MRI image classification for tumor detection using integrated hybrid convolutional k-nearest neighbor model," *J. Soft Comput. Data Mining*, vol. 5, no. 2, pp. 83–95, 2024. [CrossRef] [Google Scholar] [Publisher Link]
25. K. Kumar, K. Jyoti, and K. Kumar, "Machine learning for brain tumor classification: Evaluating feature extraction and algorithm efficiency," *Discover Artificial Intelligence*, vol. 4, no. 1, Art. no. 112, 2024. [CrossRef] [Google Scholar] [Publisher Link]
26. M. A. Al-Azawi, "Symmetry-based brain abnormality identification in magnetic resonance images," *Multimedia Tools Appl.*, vol. 82, no. 2, pp. 2563–2586, 2023. [CrossRef] [Google Scholar] [Publisher Link]
27. M. I. Mahmud, M. Mamun, and A. Abdelgawad, "A deep analysis of brain tumor detection from MR images using deep learning networks," *Algorithms*, vol. 16, no. 4, Art. no. 176, 2023. [CrossRef] [Google Scholar] [Publisher Link]
28. M. Woźniak, J. Siłka, and M. Wieczorek, "Deep neural network correlation learning mechanism for CT brain tumor detection," *Neural Comput. Appl.*, vol. 35, no. 20, pp. 14611–14626, 2023. [CrossRef] [Google Scholar] [Publisher Link]
29. H. A. Khalil, S. Darwish, Y. M. Ibrahim, and O. F. Hassan, "3D-MRI brain tumor detection model using modified level set segmentation based on dragonfly algorithm," *Symmetry*, vol. 12, no. 8, Art. no. 1256, 2020. [CrossRef] [Google Scholar] [Publisher Link]
30. T. Dudeja, S. K. Dubey, and A. K. Bhatt, "Ensembled EfficientNetB3 architecture for multi-class classification of tumours in MRI images," *Intell. Decis. Technol.*, vol. 17, no. 2, pp. 395–414, 2023. [CrossRef] [Google Scholar] [Publisher Link]
31. G. D. Kumar and S. N. Mohanty, "Brain tumor detection based on multiple deep learning models for MRI images," *EAI Endorsed Trans. Pervasive Health Technol.*, vol. 10, 2024. [CrossRef] [Google Scholar] [Publisher Link]
32. J. Zhang, X. Tan, W. Chen, G. Du, Q. Fu, H. Zhang, and H. Jiang, "EFF_D_SVM: A robust multi-type brain tumor classification system," *Frontiers in Neuroscience*, vol. 17, Art. no. 1269100, 2023. [CrossRef] [Google Scholar] [Publisher Link]
33. S. V. Rubio, M. T. García-Ordás, O. G. O. Olivera, H. Alaiz-Moretón, M. I. González-Alonso, and J. A. Benítez-Andrades, "Survival and grade of glioma prediction using transfer learning," *PeerJ Comput. Sci.*, vol. 9, Art. no. e1723, 2023. [CrossRef] [Google Scholar] [Publisher Link]
34. M. A. Mahjoubi, S. Hamida, O. E. Gannour, B. Cherradi, A. E. Abbassi, and A. Raihani, "Improved multiclass brain tumor detection using convolutional neural networks and magnetic resonance imaging," *Int. J. Adv. Comput. Sci. Appl.*, vol. 14, no. 3, 2023. [CrossRef] [Google Scholar] [Publisher Link]
35. O. Turk, D. Ozhan, E. Acar, T. C. Akinci, and M. Yilmaz, "Automatic detection of brain tumors using ensemble deep learning architectures and class activation maps," *Z. Med. Phys.*, vol. 34, no. 2, pp. 278–290, 2024. [CrossRef] [Google Scholar] [Publisher Link]
36. Kaggle Dataset, "Brain tumor detection MRI," 2024. [Online]. Available: *Kaggle* [CrossRef] [Google Scholar] [Publisher Link]